A highly sensitive strand-specific multiplex RT-qPCR assay for quantitation of Zika virus replication

Trisha R. Barnard[a], Alex B. Wang[a], and Selena M. Sagan[a,b,#]

[a]Department of Microbiology & Immunology, McGill University, Montreal, Quebec, Canada

[b]Department of Biochemistry, McGill University, Montreal, Quebec, Canada

[#]To whom correspondence should be addressed: selena.sagan@mcgill.ca

Running Title: Strand-specific quantitation of Zika virus RNA

Keywords: Reverse transcription-quantitative PCR (RT-qPCR), Strand-specific, Zika virus, RNA virus

Abstract

Reverse-transcription quantitative polymerase chain reaction (RT-qPCR) is widely used to quantify viral RNA genomes for diagnostics and research, yet conventional RT-qPCR protocols are unable to accurately distinguish between the different viral RNA species that exist during infection. Here we show that false-priming and self-priming occur during reverse transcription with several published Zika virus (ZIKV) primer sets. We developed a RT-qPCR assay using tagged primers and thermostable reverse transcriptase, which greatly reduced the occurrence of nonspecific cDNA products. Furthermore, we optimized the assay for use in multiplex qPCR which allows for simultaneous quantitative detection of positive-strand and negative-strand ZIKV RNA along with an internal control from both human and mosquito cells. Importantly, this assay is sensitive enough to study early stages of virus infection *in vitro*. Strikingly, using this assay, we detected ZIKV negative-strand RNA as early as 3 h post-infection in mammalian cell culture, at a time point prior to the onset of positive-strand RNA synthesis. Overall, the strand-specific RT-qPCR assay developed herein is a valuable tool to quantify ZIKV RNA and to study viral replication dynamics during infection. The application of these findings has the potential to increase accuracy of RNA detection methods for a variety of viral pathogens.

Highlights

- Self-primed cDNA is amplified by widely-used ZIKV qPCR primer sets
- Use of tagged primers and thermostable RT increases strand-specificity for RT-qPCR
- Multiplexed qPCR allows for simultaneous quantitation of (+) and (-) strand viral RNAs, and an internal control
- Strand-specific RT-qPCR can detect fewer than one copy of viral RNA per cell in human and mosquito cells

1. Introduction

Zika virus (ZIKV) is a mosquito-borne positive-sense RNA virus and member of the *flavivirus* genus in the *Flaviviridae* family (1). ZIKV infections are causally linked with congenital neurological complications, and ZIKV has caused a series of outbreaks of increasing severity in the past 15 years (2). Like all positive-sense RNA viruses, ZIKV replication proceeds through a negative-strand replication intermediate. New positive-strands are synthesized from the negative-strand template, and positive-strand synthesis generally outnumbers negative-strand synthesis by ~10-100 fold (3-6). Negative-strand RNA detection is therefore the gold standard for detection of ZIKV replication.

Despite being a widely used method for quantification of viral RNA, standard reverse transcription quantitative polymerase chain reaction (RT-qPCR) protocols are unable to distinguish between the multiple species of viral RNA present in a sample. As a result, standard RT-qPCR protocols are unable to determine the absolute quantity of viral genomes due to the presence of both positive- and negative-strand viral RNA (7-10). False priming of the incorrect strand, self-priming by secondary structures in the viral RNA template, or random priming by contaminating nucleic acids have been proposed to contribute to the lack of strand-specificity in standard RT-qPCR assays (11-16). Strategies to improve specificity of RT-qPCR have been developed for multiple RNA viruses, and typically involve one or more of the following: 1) use of tagged RT primers containing a unique non-viral "tag" sequence at the 5′ end of a viral-specific sequence, and the use of tag-specific primers in qPCR; 2) high-temperature RT to minimize RNA template secondary structure, or the use of a reverse transcriptase with increased specificity; or 3) purification of complementary DNA (cDNA) products to avoid excess primer carry-over into the qPCR reaction (7, 8, 10, 17). Tagged primers have been successfully used for

the strand-specific detection of some members of the *Flaviviridae* family (6, 7). However, previously-published assays for ZIKV negative-strand detection either do not use tagged primers (18-23) or have not demonstrated adequate strand-specificity (24-28). Additionally, although the use of DNA hydrolysis probes has been shown to improve the dynamic range of strand-specific qPCR, many previously-published strand-specific assays use intercalating dye chemistry (e.g. SYBR) for real-time detection in qPCR. Intercalating dyes detect all double-stranded nucleic acid non-specifically, and therefore multiple targets cannot be distinguished in a single PCR reaction (29-31). In contrast, detection of PCR amplification using hydrolysis probes can enable the detection of multiple targets from the same sample and would therefore allow for simultaneous detection of positive- and negative-strand viral RNAs, with normalization to an internal control.

Herein, we show that conventional RT-qPCR of ZIKV RNA generates cDNA from self- and false-priming. We show that both tagged primers and high-temperature RT are required to eliminate self-priming of ZIKV RNA. To further improve the utility of the strand-specific assay, we developed fluorescent probes which allowed for simultaneous detection of positive- and negative-strand viral RNAs, with an internal control. This multiplexed RT-qPCR assay is both more sensitive and specific than previously-published assays for *Flaviviridae* strand-specific RNA detection. Using this assay, we demonstrate that negative-strand ZIKV RNA can be detected in both mammalian and mosquito cells, as early as 3-6 h post-infection in cell culture.

2. Materials and methods

2.1 In vitro transcription – standard curve generation.

An infectious cDNA of ZIKV strain PRVAC59 ($ZIKV^{PR}$; Genbank accession: KX377337) was kindly provided by Young-Min Lee (Utah State University) (32). To generate the template for positive-strand RNA transcription, the ZIKV infectious cDNA was linearized with BarI (Sibenzyme), verified by agarose gel electrophoresis, and column-purified using the Zymo DNA clean & concentrator kit (Zymogen) following the manufacturer's instructions. To generate the negative-strand RNA IVT template, a T7 promoter was added to the negative-strand of the ZIKV infectious cDNA by PCR with Q5 DNA polymerase (New England Biolabs (NEB)) using primers T7-5´ZIKV(-)strand-FOR (5´-TAA TAC GAC TCA CTA TAG AGA CCC ATG GAT TTC CCC-3´) and 3´ZIKV(-)strand-REV (5´-AGT TGT TGA TCT GTG TGA ATC AG-3´). The PCR product was verified by agarose gel electrophoresis and PCR purified (Qiagen) prior to use as template in the IVT reaction. Two-hundred and fifty nanograms of linearized plasmid (positive-strand) or 150 ng PCR product (negative-strand) was used as a template in a run-off *in vitro* transcription reaction with SP6 RNA polymerase (NEB; positive-strand) or T7 RNA polymerase (NEB; negative-strand) following the manufacturer's instructions with final NTP concentration of 1 mM. The *in vitro* transcribed RNA was treated with DNase I (NEB) and analyzed by agarose gel electrophoresis prior to purification with the Zymo RNA clean & concentrator kit (Zymogen) and the concentration was determination by UV-Vis spectrophotometry at 260 nm (Nanodrop).

3.2 Primer design

In order to facilitate strand-specific detection in a multiplex assay, we designed two sets of tagged primers with separate hydrolysis probes, which would enable us to detect both positive- and negative-strands simultaneously from the same sample, with an internal control. Tagged

primers for the amplification of the negative-strand were chosen based on a previously published ZIKV RT-qPCR assay (26), and modified to match the nucleotide sequence of Asian lineage ZIKV isolates. Primers for the amplification of the positive-strand were selected such that their melting temperature was similar to those used for negative-strand detection, the amplicon was only present on genomic RNA (and not subgenomic flavivirus RNA), and that it was separated from the negative-strand by several kilobases (kb) so as to ensure specificity of probe binding to each RT product. The tag added to the positive-strand primers was adapted from (17). Mixed bases were included as needed to ensure primers were complementary to multiple ZIKV isolates. For the internal control (Glyceraldehyde 3-phosphate dehydrogenase (GAPDH)), primers were modified from (33) such that their melting temperature was similar to the ZIKV primers. Primers for mosquito GAPDH detection were designed with IDT's PrimerQuest tool based on *Aedes aegypti* glyceraldehyde-3-phosphate dehydrogenase mRNA (XM_011494724.2; XM_019687453.2) All qPCR probes were designed using IDT's PrimerQuest tool. All primer/probe sequences (listed in **Tables 1 and 2)** were checked for self-complementarity and potential heterodimerization using IDT's oligoanalyzer tool.

2.3 Standard RT-qPCR

RNA was mixed with 2 pmol of each primer (**Table 1, Figure 1**) and 0.5 mM dNTPs, denatured at 95 °C for 5 min and then immediately transferred to ice, where the RT buffer, DTT, RNase inhibitor (SuperasIN, Invitrogen or Ribolock, Thermo Scientific), and 0.5 μL SuperScript III reverse transcriptase (Invitrogen) were added as per the manufacturer's instructions. RNA was then incubated at 55 °C for 30 min and the reaction was heat-inactivated at 70 °C for 15 min. Ten percent of the cDNA volume was used in the qPCR reaction. Quantitative PCR of the

132 samples reverse transcribed using primers from Lanciotti *et al*. was performed using iTaq
133 universal probes supermix (BioRad) with 300 nM each of the primers and probe (34).
134 Thermocycling conditions were: 95ºC 3 min, followed by 40 cycles of: 95ºC 15 sec, 60ºC 60 sec
135 + plate read. Quantitative PCR of the samples reverse transcribed with primers from Balm *et al*.
136 was performed using SuperScript III Platinum SYBR Green One-Step qRT-PCR Kit (Invitrogen)
137 with 200 nM primers and omitting the RT step (35). Thermocycling conditions were: 94 ºC 2
138 min, followed by 40 cycles of: 94 ºC 15 sec, 60 ºC 30 sec, 68 ºC 15 sec + plate read, followed by
139 a Meltcurve from 65 ºC to 95 ºC. All qPCR reactions were performed on a CFX96 thermocycler
140 (BioRad).
141
142 *2.4 Strand-specific RT-qPCR*
143 RNA was mixed with 10 nM each RT primer (**Table 2**) and 5 μM dNTPs, denatured at 95 °C for
144 5 min then immediately transferred to ice, where the RT buffer and RNase inhibitor (SuperasIN,
145 Invitrogen or Ribolock, Thermo Scientific) were added. RNA was then transferred to 60 °C, after
146 which 0.5 μL Maxima H-minus reverse transcriptase (Thermo Scientific) was added and the
147 temperature was immediately transferred to 65 °C for 30 min. The RT reaction was heat-
148 inactivated at 85 °C for 5 min and the cDNA was purified using the Zymo DNA clean &
149 concentrator kit (Zymogen) according to the manufacturer's instructions for cDNA clean-up.
150 Quantitative PCR was performed using iTaq universal probes supermix (BioRad) with primer
151 concentrations listed in **Table 3.** Thermocycling conditions were: 95 ºC 2 min, followed by 45
152 cycles of: 95 ºC 15 sec, 64 ºC 30 sec + plate read. For RNA extracted from mosquito cells,
153 thermocycling conditions were: 95 ºC 2 min, followed by 45 cycles of: 95 ºC 15 sec, 64 ºC 60
154 sec + plate read to improve mosquito GAPDH PCR efficiency. ZIKV RNA was quantified

based on a standard curve of *in vitro* transcribed positive- and negative-strand genomes, and was normalized to GAPDH by a modified ΔCt method (36).

2.5 Cell culture

Human lung carcinoma (A549) cells, kindly provided by Russell Jones (Van Andel Institute, Michigan, U.S.A.), were maintained in Dulbecco's modified Eagle's medium (DMEM, Wisent Inc.) supplemented with 10% fetal bovine serum (FBS, Wisent Inc.), 1% Non-essential amino acids (Wisent Inc.), 1% L-glutamine (Wisent Inc.), and 1% penicillin/streptomycin (Wisent Inc.) at 37 °C/5 % CO_2. Human choriocarcinoma (JEG-3) cells, kindly provided by Eric Miska (University of Cambridge, Cambridge, U.K.), were maintained in Eagle's minimum essential medium (EMEM; Wisent Inc.) supplemented with 10% FBS, 1% Non-essential amino acids, 1% L-glutamine, 1% penicillin/streptomycin, and 1 mM sodium pyruvate (Wisent Inc.) at 37 °C/5% CO_2. *Aedes albopictus* (C6/36) cells (ATCC) were maintained in Eagle's minimum essential medium (EMEM; Wisent Inc.) supplemented with 10% FBS, 1% Non-essential Amino acids, 1% L-glutamine, 1% Pen/Strep, and 15 mM HEPES (Wisent Inc.) at 28 °C/5 % CO_2.

2.6 Virus infections

An infectious cDNA of ZIKV strain PRVAC59 (Genbank accession: KX377337) was kindly provided by Young-Min Lee (Utah State University) (32). Viral stocks were generated by transfection of Vero cells with *in vitro* transcribed ZIKV RNA as previously described, followed by a single passage in Vero cells (37). Viral stocks were diluted to the indicated MOI in EMEM and were allowed to bind to subconfluent monolayers of cells for 1 h at 37 °C/5 % CO_2, after which the inoculum was removed, cells were washed once with PBS, and media was replaced

with fresh media containing 15 mM HEPES and 2% FBS. At the indicated time points post-infection, RNA was harvested in TriZol (Invitrogen) and extracted following the manufacturer's instructions. Five-hundred nanograms of total RNA was used in the multiplex strand-specific RT-qPCR protocol.

3. Results

3.1 Conventional RT-qPCR is not strand-specific.

We performed standard two-step RT-qPCR on *in vitro* transcribed ZIKV RNA positive- and negative-strand RNA using two previously published and widely used ZIKV primer sets (**Figure 1** and **Table 1**) (34, 35). We used different primers in the reverse transcription reaction to evaluate the potential contributions of false- and self-priming on the specific signal generated with the correct RT primer to detect the indicated strand. For specific priming, the reverse primer was used to reverse transcribe the positive-strand viral RNA, and the forward primer was used to reverse transcribe the negative-strand viral RNA. For false priming, the forward primer was used to reverse transcribe the positive-strand viral RNA, and the reverse primer was used to reverse transcribe the negative-strand viral RNA. For self-priming, no primers were added to the reverse transcription reaction. For both positive- and negative-strand viral RNA, both self- and false-priming occurred and was detectable when even as few as 10^3 RNA copies were added to the RT reaction (**Figure 1**). Notably, there did not appear to be a difference in the degree of incorrectly primed cDNA products between the two chosen primer sets, even though they anneal to different regions of the viral genome. These results indicate that conventional RT-qPCR using several published ZIKV primer sets yields incorrectly-primed cDNA products and is therefore not suitable for quantitative strand-specific detection of viral RNAs.

3.2 Tagged primers with modified RT conditions largely eliminate false- and self-priming

We next tested whether the use of tagged primers would improve specificity**.** We designed tagged primers to specifically detect both positive- and negative-strand ZIKV RNA (**Figure 2A** and **Tables 2 and 3,** see **Materials and methods**). Although tagged primers have been widely reported to improve strand specificity, we found that tagged primers used alone in a standard RT-qPCR set-up did not sufficiently eliminate self- and false-priming of cDNA products (**Figure 2B-C**). To improve specificity, we purified cDNA products prior to qPCR analysis to remove any excess primer. We also increased the RT temperature, which required the use of a thermostable reverse transcriptase. We found that these conditions completely eliminated self-priming and greatly reduced the occurrence of false-priming (**Figure 2D-E**).

3.3 Multiplex qPCR optimization

We next wanted to develop qPCR primers and probes which would enable us to multiplex detection of positive- and negative-strand viral RNAs together with an internal control (see **Materials and methods**). Given that there is reported to be up to 100-fold excess of positive-strand compared with negative-strand viral RNA during ZIKV infection, we first determined whether the primer concentrations needed for accurate detection of the negative-strand in multiplex PCR would need optimization (3-6). In a multiplex qPCR assay, it is important to verify that the amplification of high-abundance targets does not interfere with detection of low-abundance targets by depleting reagents (e.g. dNTPs, polymerase) at early cycles. Indeed, we found that when strand-specific cDNA from ZIKV-infected cells was subject to multiplex qPCR using typical qPCR primer concentrations (300 nM) for both positive- and negative-strand

224 detection, detection of negative-strands was severely impaired (**Figure 3A**). This problem can be
225 circumvented by modifying the primer concentration of high-abundance targets such that primers
226 become limiting for that target (**Figure 3A**). The optimal primer concentrations necessary for
227 accurate multiplex qPCR detection of all targets is provided in **Table 3**.

228 Moreover, we showed that the addition of ZIKV RNA does not affect amplification of
229 the housekeeping gene used as internal control (GAPDH) (**Figure 3B**), and that the addition of
230 total RNA does not affect ZIKV amplification (**Figure 3C-D**). Importantly, GAPDH PCR
231 efficiency is similar to ZIKV PCR efficiency (see section 3.5), so a modified ΔCt method could
232 be used for normalization to the internal control (36). Similar optimization was performed for
233 detection of ZIKV RNAs and an internal control RNA in mosquito cells (**Figure S1**). Finally, we
234 validated the choice of housekeeping gene by determining that ZIKV infection does not affect
235 GAPDH expression in both human and mosquito cells (**Figure S2**). Overall, these results suggest
236 that the multiplex RT-qPCR assay can be used to accurately quantify ZIKV RNA from infected
237 cells.
238
239 *3.4 Demonstration of strand-specificity of the multiplex RT-qPCR assay*
240 To determine the strand-specificity of the multiplex RT-qPCR assay, we mixed *in vitro*
241 transcribed ZIKV positive- or negative-strand RNA with 100-fold, 1,000-fold, or 10,000-fold
242 excess of the opposite strand (**Figure 4**). We found that positive-strand ZIKV RNA detection
243 was specific up to at least 100-fold excess negative-strand RNA, after which excess negative-
244 strands interfered with positive-strand detection (**Figure 4A**). Negative-strand RNA detection
245 was specific up to at least 1000-fold excess positive-strand RNA, beyond which excess positive-
246 strands could be non-specifically detected by the negative-strand assay (**Figure 4B**).

247

248 *3.5 Validation of the strand-specific multiplex RT-qPCR assay*

249 We next evaluated the sensitivity and reproducibility of the assay using *in vitro* transcribed
250 positive- and negative-strand ZIKV RNA. A representative standard curve, consisting of 10-fold
251 serial dilutions of 2.5×10^8 copies each of positive- and negative-strands, was repeatedly
252 subjected to the strand-specific multiplex RT-qPCR assay (**Figure 5**). Detection of positive- and
253 negative-strands was similar across all dilutions. The standard deviation of each dilution was on
254 average 1.73 Ct values for the positive-strand and 1.82 Ct values for the negative-strand, and did
255 not vary across dilutions (see coefficient of variation (%CV) values in **Table 4**). The PCR
256 efficiency averaged 92.9 ± 3.4% (R^2 value of 0.980-0.999) and 90.1% ± 8.0% (R^2 value of
257 0.989-0.998) for positive- and negative-strand detection, respectively. GAPDH PCR efficiency
258 was 91.2 ± 5.8% (R^2 value of 0.944-0.987). The lower limit of quantitation (LLOQ) ranged from
259 134 – 333 and 130 – 2109 copies per reaction for the positive- and negative-strand, respectively.
260 Given that up to 500 ng RNA was analyzed per reaction, this represents a lower limit of
261 quantitation of 0.27-0.67 and 0.26-4.22 positive- and negative-strand copies per ng RNA,
262 respectively.

263

264 *3.6 Quantitation of positive- and negative-strand ZIKV RNA in cell culture*

265 In order to understand ZIKV replication dynamics in cell culture, the strand-specific RT-qPCR
266 assay was used to quantify ZIKV RNA in infected cells. We performed one-step kinetics in
267 human placental choriocarcinoma (JEG-3) cells infected with ZIKV (**Figure 6A**). Interestingly,
268 we found that negative-strand RNA could be detected as early as 3 h post-infection.
269 Correspondingly, positive-strand RNA began to increase between 3 and 6 h post-infection, again

implying that negative-strands were synthesized by this time point. Both positive- and negative-strand RNA continued to increase throughout the duration of experiment, indicating that active viral replication was occurring. The (+):(-) RNA ratio was approximately 30-60:1 at all timepoints where negative-strand RNA could be quantified.

Similarly, active viral replication was also detectable in C6/36 mosquito cells (**Figure 6B**). We found that ZIKV positive- and negative-strand RNAs increased throughout the duration of the experiment, suggesting that active viral replication was occurring. Interestingly, even at very low MOIs (i.e. MOI = 0.01), negative-strand RNA could be detected as early as 24 h post-infection. In mosquito cells, the (+):(-) RNA ratio was approximately 30-50:1. Overall, our results demonstrate that the strand-specific RT-qPCR assay can be used to quantify ZIKV positive- and negative-strand RNA from both human and mosquito cells.

4. Discussion

Herein, we show that incorrectly-primed cDNA products are generated during reverse transcription with commonly-used ZIKV primer sets. Consequently, we developed a strand-specific multiplexed RT-qPCR assay for the quantitation of ZIKV RNA in infected human and mosquito cells. We show that the assay provides sufficient specificity for detection of positive- and negative-strand ZIKV RNA during infection. Finally, we demonstrate that the assay can be multiplexed and used to quantify ZIKV RNA replication in both human and mosquito cells. In summary, the strand-specific RT-qPCR assay developed herein is a useful tool for the evaluation of ZIKV RNA replication kinetics, tropism, and persistence in both human and mosquito cells.

Interestingly, the majority of the nonspecific priming observed during conventional RT-qPCR was due to self-priming of the viral RNA. There is a high degree of secondary structure

observed throughout the ZIKV genome, which may contribute to self-primed cDNA synthesis (38, 39). The degree of self-priming did not differ between the two primer sets, despite their specificity for different regions of the viral genome. This suggests that self-priming occurs throughout the ZIKV genome, and should be considered when performing RT on ZIKV RNA. Furthermore, the genomes of diverse RNA viruses are highly structured, and as such self-priming is likely to be a problem for strand-specific RNA detection of multiple viral families (40-42). Indeed, self-priming during RT has been demonstrated to occur for numerous RNA viruses, including Dengue virus, hepatitis E virus, human rhinovirus, hepatitis C virus, and several plant RNA viruses (16, 43-46).

Importantly, use of tagged primers with high-temperature RT completely eliminated self-priming, which constituted the majority of nonspecific events. Despite this, the limit of strand-specificity for negative-strand detection was 1000-fold excess positive-strands. This is likely due to small degree of false priming that could still be detected even with tagged primers. Interestingly, although false priming of the positive-strand occurred to a similar degree, 1000-fold excess negative-strand decreased rather than increased signal, suggesting that the excess negative-strand impeded positive-strand detection, likely through hybridization with complementary RNA. Other strand-specific RT-qPCR assays using tagged primers have reported complete specificity (i.e. no detection of even very high amounts of the incorrect strand), suggesting that further modification of our tagged primers has the potential to further improve specificity. However, higher specificity likely comes as a trade-off to sensitivity (7). Increased specificity, i.e. beyond 1000:1 (+):(-) RNA, is likely unnecessary as the (+):(-) RNA ratio during infection is within our assay's range of specificity, where a ratio of 10:1-100:1 excess positive-strand RNA has been reported (3-6). Furthermore, decreased sensitivity would impede negative-

316 strand detection at early time points and render the assay less able to quantify early events in
317 viral replication.

318 Although both viral RNA targets were detected similarly, PCR efficiency was more
319 variable in the negative-strand assay than the positive-strand assay. This was likely due to
320 stochastic detection of the lowest concentration of negative-strand RNA standards (47), as
321 indicated by the greater degree of variability of the negative- vs. positive-strand LLOQ, rather
322 than overall greater variability of negative-strand detection as the standard deviation of each Ct
323 did not vary between (+) and (-) RNA. PCR efficiency between 90-110% is generally considered
324 acceptable, and both positive- and negative-strand detection fell within this range (48). It is
325 possible that this variability in efficiency of negative-strand detection was caused by the quality
326 of the *in vitro* transcribed RNA transcripts used in the experimental determination of PCR
327 efficiency.

328 Despite the above-described limitations, to our knowledge this assay represents the first
329 validation of a strand-specific multiplex RT-qPCR assay for ZIKV RNA quantitation. The assay
330 presented herein improves over similar previously validated *flavivirus* strand-specific RT-qPCR
331 assays, which are not sensitive enough to quantify early events in viral replication (7).
332 Depending on the amount of input RNA added to the RT reaction, the lower limit of quantitation
333 of ~200-2000 copies/reaction can be as low as 0.5-5 copies per ng input RNA. Estimates suggest
334 that a single mammalian cell contains approximately 10-20 pg total RNA (49); as such, the lower
335 limit of detection of our assay is less than one copy of viral RNA per cell. Thus, this enables the
336 study of very early events in the viral life cycle.

337 Mosquitoes are an important component of the ZIKV transmission cycle and therefore
338 the study of viral replication in mosquitoes may provide insights into potential strategies to block

transmission. To our knowledge, detection of ZIKV negative-strand RNA from either mosquito cells in culture or live mosquitoes is rare (50). Nonetheless, the assay developed herein allows quantification of ZIKV replication in mosquito cells and could potentially be used to quantify viral replication from mosquito tissues, which would expand our knowledge of transmission bottlenecks and mechanisms of viral replication in the insect vector.

Overall, this study adds to the growing body of evidence which suggests that conventional RT-qPCR methods do not accurately detect viral genomes in the presence of other forms of viral RNA (7, 8, 10, 51-53). Results from studies that present strand-specific RT-qPCR data in the absence of a validated strand-specific assay should therefore be interpreted with the caveat that one cannot necessarily conclude that RNA copy number represents uniquely genomic or antigenomic RNA. For viruses which make multiple mRNA species in addition to genomic and antigenomic RNA (e.g. Coronaviruses), conventional RT-qPCR is perhaps even less likely to provide accurate quantitation of viral genomic RNAs. Importantly, similar limitations of strand-specific detection are not limited to positive-sense RNA viruses (9, 51, 52). Nevertheless, with some thought it is possible to design strategies to specifically detect the RNA species of interest even in the presence of several types of viral RNA (51, 52, 54, 55).

Acknowledgements

We thank Young-Min Lee (Utah State University) for providing ZIKV^{PR} infectious cDNA. We also thank Russell Jones (Van Andel Institute, Michigan, U.S.A.), and Eric Miska (University of Cambridge, Cambridge, U.K.) for providing human lung carcinoma (A549) and human choriocarcinoma (JEG-3) cells, respectively. Finally, we thank Quinn Abram for providing RNA from infected C6/36 cells.

Funding Information

This research was supported by the Canadian Institutes of Health Research (CIHR) project grant program [PJT-162212, S.M.S.] and NSERC Discovery grant program [RGPIN-2020-04713, S.M.S.]. T.R.B is supported by a doctoral training award (CGS-D) from the Fonds de recherche du Québec - Santé (FRQS). In addition, this research was undertaken, in part, thanks to the Canada Research Chairs program (S.M.S). The funders had no role in study design, data collection and analysis, decision to publish, or preparation of the manuscript.

Author Contributions

T.R.B and S.M.S designed the study; T.R.B. and A.B.W performed the experiments and analyzed the data, and T.R.B. wrote and edited the manuscript with assistance from S.M.S. and A.B.W.

References

1. Simmonds P, Becher P, Bukh J, Gould EA, Meyers G, Monath T, Muerhoff S, Pletnev A, Rico-Hesse R, Smith DB, Stapleton JT, Ictv Report C. 2017. ICTV Virus Taxonomy Profile: Flaviviridae. J Gen Virol 98:2-3.
2. Gubler DJ, Vasilakis N, Musso D. 2017. History and Emergence of Zika Virus. J Infect Dis 216:S860-S867.
3. Choi KH. 2021. The Role of the Stem-Loop A RNA Promoter in Flavivirus Replication. Viruses 13.
4. Hodge K, Kamkaew M, Pisitkun T, Chimnaronk S. 2019. Flavors of Flaviviral RNA Structure: towards an Integrated View of RNA Function from Translation through Encapsidation. Bioessays 41:e1900003.
5. Kim YG, Yoo JS, Kim JH, Kim CM, Oh JW. 2007. Biochemical characterization of a recombinant Japanese encephalitis virus RNA-dependent RNA polymerase. BMC Mol Biol 8:59.
6. Raquin V, Lambrechts L. 2017. Dengue virus replicates and accumulates in Aedes aegypti salivary glands. Virology 507:75-81.

7. Lim SM, Koraka P, Osterhaus AD, Martina BE. 2013. Development of a strand-specific real-time qRT-PCR for the accurate detection and quantitation of West Nile virus RNA. J Virol Methods 194:146-53.
8. Plaskon NE, Adelman ZN, Myles KM. 2009. Accurate strand-specific quantification of viral RNA. PLoS One 4:e7468.
9. Purcell MK, Hart SA, Kurath G, Winton JR. 2006. Strand-specific, real-time RT-PCR assays for quantification of genomic and positive-sense RNAs of the fish rhabdovirus, Infectious hematopoietic necrosis virus. J Virol Methods 132:18-24.
10. Vashist S, Urena L, Goodfellow I. 2012. Development of a strand specific real-time RT-qPCR assay for the detection and quantitation of murine norovirus RNA. J Virol Methods 184:69-76.
11. Gunji T, Kato N, Hijikata M, Hayashi K, Saitoh S, Shimotohno K. 1994. Specific detection of positive and negative stranded hepatitis C viral RNA using chemical RNA modification. Arch Virol 134:293-302.
12. Haddad F, Qin AX, Giger JM, Guo H, Baldwin KM. 2007. Potential pitfalls in the accuracy of analysis of natural sense-antisense RNA pairs by reverse transcription-PCR. BMC Biotechnol 7:21.
13. Lanford RE, Sureau C, Jacob JR, White R, Fuerst TR. 1994. Demonstration of in vitro infection of chimpanzee hepatocytes with hepatitis C virus using strand-specific RT/PCR. Virology 202:606-14.
14. Peyrefitte CN, Pastorino B, Bessaud M, Tolou HJ, Couissinier-Paris P. 2003. Evidence for in vitro falsely-primed cDNAs that prevent specific detection of virus negative strand RNAs in dengue-infected cells: improvement by tagged RT-PCR. Journal of Virological Methods 113:19-28.
15. Timofeeva AV, Skrypina NA. 2001. Background activity of reverse transcriptases. Biotechniques 30:22-4, 26, 28.
16. Tuiskunen A, Leparc-Goffart I, Boubis L, Monteil V, Klingstrom J, Tolou HJ, Lundkvist A, Plumet S. 2010. Self-priming of reverse transcriptase impairs strand-specific detection of dengue virus RNA. J Gen Virol 91:1019-27.
17. Grunvogel O, Colasanti O, Lee JY, Kloss V, Belouzard S, Reustle A, Esser-Nobis K, Hesebeck-Brinckmann J, Mutz P, Hoffmann K, Mehrabi A, Koschny R, Vondran FWR, Gotthardt D, Schnitzler P, Neumann-Haefelin C, Thimme R, Binder M, Bartenschlager R, Dubuisson J, Dalpke AH, Lohmann V. 2018. Secretion of Hepatitis C Virus Replication Intermediates Reduces Activation of Toll-Like Receptor 3 in Hepatocytes. Gastroenterology 154:2237-2251 e16.
18. Sun X, Hua S, Chen H-R, Ouyang Z, Einkauf K, Tse S, Ard K, Ciaranello A, Yawetz S, Sax P, Rosenberg ES, Lichterfeld M, Yu XG. 2017. Transcriptional Changes during Naturally Acquired Zika Virus Infection Render Dendritic Cells Highly Conducive to Viral Replication. Cell Reports 21:3471-3482.
19. Papa MP, Meuren LM, Coelho SVA, Lucas CGdO, Mustafá YM, Lemos Matassoli F, Silveira PP, Frost PS, Pezzuto P, Ribeiro MR, Tanuri A, Nogueira ML, Campanati L, Bozza MT, Paula Neto HA, Pimentel-Coelho PM, Figueiredo CP, Aguiar RSd, Arruda LBd. 2017. Zika Virus Infects, Activates, and Crosses Brain Microvascular Endothelial Cells, without Barrier Disruption. Frontiers in Microbiology 8.

20. Barnard TR, Rajah MM, Sagan SM. 2018. Contemporary Zika Virus Isolates Induce More dsRNA and Produce More Negative-Strand Intermediate in Human Astrocytoma Cells. Viruses 10.
21. Bayer A, Lennemann NJ, Ouyang Y, Bramley JC, Morosky S, Marques ET, Jr., Cherry S, Sadovsky Y, Coyne CB. 2016. Type III Interferons Produced by Human Placental Trophoblasts Confer Protection against Zika Virus Infection. Cell Host Microbe 19:705-12.
22. Barbeito-Andrés J, Pezzuto P, Higa LM, Dias AA, Vasconcelos JM, Santos TMP, Ferreira JCCG, Ferreira RO, Dutra FF, Rossi AD, Barbosa RV, Amorim CKN, Souza MPCD, Chimelli L, Aguiar RS, Gonzalez PN, Lara FA, Castro MC, Molnár Z, Lopes RT, Bozza MT, Vianez JLSG, Barbeito CG, Cuervo P, Bellio M, Tanuri A, Garcez PP. 2020. Congenital Zika syndrome is associated with maternal protein malnutrition. Science Advances 6:eaaw6284.
23. Gavino-Leopoldino D, Figueiredo CM, Silva MOLd, Barcellos LG, Neris RLS, Pinto LDM, Araújo SMB, Ladislau L, Benjamim CF, Poian ATD, Clarke JR, Figueiredo CP, Assunção-Miranda I, Heise MT. 2021. Skeletal Muscle Is an Early Site of Zika Virus Replication and Injury, Which Impairs Myogenesis. Journal of Virology 95:e00904-21.
24. Robinson CL, Chong ACN, Ashbrook AW, Jeng G, Jin J, Chen H, Tang EI, Martin LA, Kim RS, Kenyon RM, Do E, Luna JM, Saeed M, Zeltser L, Ralph H, Dudley VL, Goldstein M, Rice CM, Cheng CY, Seandel M, Chen S. 2018. Male germ cells support long-term propagation of Zika virus. Nat Commun 9:2090.
25. Li X-F, Dong H-L, Huang X-Y, Qiu Y-F, Wang H-J, Deng Y-Q, Zhang N-N, Ye Q, Zhao H, Liu Z-Y, Fan H, An X-P, Sun S-H, Gao B, Fa Y-Z, Tong Y-G, Zhang F-C, Gao GF, Cao W-C, Shi P-Y, Qin C-F. 2016. Characterization of a 2016 Clinical Isolate of Zika Virus in Non-human Primates. EBioMedicine 12:170-177.
26. Liu D, Tedbury PR, Lan S, Huber AD, Puray-Chavez MN, Ji J, Michailidis E, Saeed M, Ndongwe TP, Bassit LC, Schinazi RF, Ralston R, Rice CM, Sarafianos SG. 2019. Visualization of Positive and Negative Sense Viral RNA for Probing the Mechanism of Direct-Acting Antivirals against Hepatitis C Virus. Viruses 11.
27. Aviner R, Li KH, Frydman J, Andino R. 2021. Cotranslational prolyl hydroxylation is essential for flavivirus biogenesis. Nature 596:558-564.
28. Zimmerman MG, Quicke KM, O'Neal JT, Arora N, Machiah D, Priyamvada L, Kauffman RC, Register E, Adekunle O, Swieboda D, Johnson EL, Cordes S, Haddad L, Chakraborty R, Coyne CB, Wrammert J, Suthar MS. 2018. Cross-Reactive Dengue Virus Antibodies Augment Zika Virus Infection of Human Placental Macrophages. Cell Host Microbe 24:731-742 e6.
29. Cao H, Shockey JM. 2012. Comparison of TaqMan and SYBR Green qPCR methods for quantitative gene expression in tung tree tissues. J Agric Food Chem 60:12296-303.
30. Jamnikar Ciglenecki U, Grom J, Toplak I, Jemersic L, Barlic-Maganja D. 2008. Real-time RT-PCR assay for rapid and specific detection of classical swine fever virus: comparison of SYBR Green and TaqMan MGB detection methods using novel MGB probes. J Virol Methods 147:257-64.
31. Soltany-Rezaee-Rad M, Sepehrizadeh Z, Mottaghi-Dastjerdi N, Yazdi MT, Seyatesh N. 2015. Comparison of SYBR Green and TaqMan real-time PCR methods for quantitative detection of residual CHO host-cell DNA in biopharmaceuticals. Biologicals 43:130-5.

32. Yun SI, Song BH, Frank JC, Julander JG, Olsen AL, Polejaeva IA, Davies CJ, White KL, Lee YM. 2018. Functional Genomics and Immunologic Tools: The Impact of Viral and Host Genetic Variations on the Outcome of Zika Virus Infection. Viruses 10.
33. Zarember KA, Godowski PJ. 2002. Tissue Expression of Human Toll-Like Receptors and Differential Regulation of Toll-Like Receptor mRNAs in Leukocytes in Response to Microbes, Their Products, and Cytokines. The Journal of Immunology 169:1136-1136.
34. Lanciotti RS, Kosoy OL, Laven JJ, Velez JO, Lambert AJ, Johnson AJ, Stanfield SM, Duffy MR. 2008. Genetic and serologic properties of Zika virus associated with an epidemic, Yap State, Micronesia, 2007. Emerg Infect Dis 14:1232-9.
35. Balm MN, Lee CK, Lee HK, Chiu L, Koay ES, Tang JW. 2012. A diagnostic polymerase chain reaction assay for Zika virus. J Med Virol 84:1501-5.
36. Livak KJ, Schmittgen TD. 2001. Analysis of relative gene expression data using real-time quantitative PCR and the 2(-Delta Delta C(T)) Method. Methods 25:402-8.
37. Shan C, Xie X, Muruato AE, Rossi SL, Roundy CM, Azar SR, Yang Y, Tesh RB, Bourne N, Barrett AD, Vasilakis N, Weaver SC, Shi PY. 2016. An Infectious cDNA Clone of Zika Virus to Study Viral Virulence, Mosquito Transmission, and Antiviral Inhibitors. Cell Host Microbe 19:891-900.
38. Li P, Wei Y, Mei M, Tang L, Sun L, Huang W, Zhou J, Zou C, Zhang S, Qin CF, Jiang T, Dai J, Tan X, Zhang QC. 2018. Integrative Analysis of Zika Virus Genome RNA Structure Reveals Critical Determinants of Viral Infectivity. Cell Host Microbe 24:875-886 e5.
39. Ziv O, Gabryelska MM, Lun ATL, Gebert LFR, Sheu-Gruttadauria J, Meredith LW, Liu ZY, Kwok CK, Qin CF, MacRae IJ, Goodfellow I, Marioni JC, Kudla G, Miska EA. 2018. COMRADES determines in vivo RNA structures and interactions. Nat Methods 15:785-788.
40. Boerneke MA, Ehrhardt JE, Weeks KM. 2019. Physical and Functional Analysis of Viral RNA Genomes by SHAPE. Annu Rev Virol 6:93-117.
41. Nicholson BL, White KA. 2015. Exploring the architecture of viral RNA genomes. Curr Opin Virol 12:66-74.
42. Smyth RP, Negroni M, Lever AM, Mak J, Kenyon JC. 2018. RNA Structure-A Neglected Puppet Master for the Evolution of Virus and Host Immunity. Front Immunol 9:2097.
43. Lerat H, Berby F, Trabaud MA, Vidalin O, Major M, Trepo C, Inchauspe G. 1996. Specific detection of hepatitis C virus minus strand RNA in hematopoietic cells. J Clin Invest 97:845-51.
44. Zhang C, Wu HN, Zhang YQ, Shen JG, Li WM. 2015. Self-priming on the plant viral RNAs during reverse transcription-PCR. Acta Virol 59:92-7.
45. Wiehler S, Proud D. 2021. Specific Assay of Negative Strand Template to Quantify Intracellular Levels of Rhinovirus Double-Stranded RNA. Methods Protoc 4.
46. Chatterjee SN, Devhare PB, Lole KS. 2012. Detection of negative-sense RNA in packaged hepatitis E virions by use of an improved strand-specific reverse transcription-PCR method. J Clin Microbiol 50:1467-70.
47. Rawer D, Borkhardt A, Wilda M, Kropf S, Kreuder J. 2003. Influence of stochastics on quantitative PCR in the detection of minimal residual disease. Leukemia 17:2527-8; author reply 2528-31.

526 48. Bustin SA, Benes V, Garson JA, Hellemans J, Huggett J, Kubista M, Mueller R, Nolan T,
527 Pfaffl MW, Shipley GL, Vandesompele J, Wittwer CT. 2009. The MIQE guidelines:
528 minimum information for publication of quantitative real-time PCR experiments. Clin
529 Chem 55:611-22.
530 49. Han F, Lillard SJ. 2000. In-situ sampling and separation of RNA from individual
531 mammalian cells. Anal Chem 72:4073-9.
532 50. da Costa CF, da Silva AV, do Nascimento VA, de Souza VC, Monteiro D, Terrazas
533 WCM, Dos Passos RA, Nascimento S, Lima JBP, Naveca FG. 2018. Evidence of vertical
534 transmission of Zika virus in field-collected eggs of Aedes aegypti in the Brazilian
535 Amazon. PLoS Negl Trop Dis 12:e0006594.
536 51. Kawakami E, Watanabe T, Fujii K, Goto H, Watanabe S, Noda T, Kawaoka Y. 2011.
537 Strand-specific real-time RT-PCR for distinguishing influenza vRNA, cRNA, and
538 mRNA. J Virol Methods 173:1-6.
539 52. Tercero B, Terasaki K, Nakagawa K, Narayanan K, Makino S. 2019. A strand-specific
540 real-time quantitative RT-PCR assay for distinguishing the genomic and antigenomic
541 RNAs of Rift Valley fever phlebovirus. Journal of Virological Methods 272:113701.
542 53. Bessaud M, Autret A, Jegouic S, Balanant J, Joffret ML, Delpeyroux F. 2008.
543 Development of a Taqman RT-PCR assay for the detection and quantification of
544 negatively stranded RNA of human enteroviruses: evidence for false-priming and
545 improvement by tagged RT-PCR. J Virol Methods 153:182-9.
546 54. Escaffre O, Queguiner M, Eterradossi N. 2010. Development and validation of four Real-
547 Time quantitative RT-PCRs specific for the positive or negative strands of a bisegmented
548 dsRNA viral genome. J Virol Methods 170:1-8.
549 55. Mancarella A, Procopio FA, Achsel T, De Crignis E, Foley BT, Corradin G, Bagni C,
550 Pantaleo G, Graziosi C. 2019. Detection of Human Immunodeficiency Virus Type 1
551 (HIV-1) Antisense Protein (ASP) RNA Transcripts in Patients by Strand-Specific RT-
552 PCR. J Vis Exp doi:10.3791/60511.
553

554

Tables

Table 1: Primers used in standard RT-qPCR

Primer	Nucleotide position	Sequence (5′-3′)	Orientation	Reference
ZIKVF9027	9121–9141	CCT TGG ATT CTT GAA CGA GGA	Forward	(35)
ZIKVR9197c	9312–9290	AGA GCT TCA TTC TCC AGA TCA A	Reverse	
ZIKV 1086	1086–1102	CCG CTG CCC AAC ACA AG	Forward	(34)
ZIKV 1162c	1162–1139	CCA CTA ACG TTC TTT TGC AGA CAT	Reverse	
ZIKV 1107-FAM	1107–1137	AGC CTA CCT TGA CAA GCA GTC AGA CAC TCA A	Probe	

Table 2: Tagged primers used in RT

Primer	Sequence (5′-3′)[a]
Pos strand RT primer (5993-Tag5-REV)	CTG GAG TCG TAG ATC CTA CCG CGT TTR TTG GGA TTC CTG CCT
Neg strand RT primer (10287-ZVtag-FOR)	GGC CGT CAT GGT GGC GAA TAA AGG ATC ATA GGT GAT GAA GAA AAG T
hsGAPDH RT primer	GCT CCT GGA AGA TGG TGA TGG GAT TTC C
AaGAPDH RT primer	CGT ACC AGG AGA TGA GCT TGA CGA AAG TG

[a]Tag sequence unique to the primer is underlined

Table 3: Primers used in multiplex strand-specific qPCR

Primer	Sequence (5′-3′)	Primer concentration in multiplex qPCR (nM)
(+)RNA FOR primer (ZVPR-5895 FOR)	AGA TGC CTA AAG CCG GTC ATA CT	75
(+)RNA REV primer (Tag5)	CTG GAG TCG TAG ATC CTA CCG C	75
(+)RNA probe (5938-5962) (Cy5)	TGG CTG GAC CCA TGC CTG TCA CAC A	75
(-) RNA FOR primer (ZIKV-tag)	GGC CGT CAT GGT GGC GAA TAA	900
(-) RNA REV primer (ZVPR-10402-REV)	CCT GAC AAC ATT AAG ATT GGT GCT TAC AG	900
(-) RNA probe (10345-10372) (FAM)	TGG GTG AAG AAG GGT CYA CAC CTG GAG T	300
hsGAPDH FOR	GGA AGG TGA AGG TCG GAG TCA ACG G	150
hsGAPDH REV	GCT CCT GGA AGA TGG TGA TGG GAT TTC C	150
hsGAPDH probe (HEX)	AGC TTC CCG TTC TCA GCC TTG AC	150
aaGAPDH FOR primer	TAC ACC GAA GAG GAG GTC GTC TCC	150
aaGAPDH REV primer	CGT ACC AGG AGA TGA GCT TGA CGA AAG TG	150
aaGAPDH probe (HEX)	TAC CCA CTC CTC CAT CTT TGA CGC C	150

566 **Table 4: Intra-assay variability**

log (RNA copies)	8	7	6	5	4	3	2
(+) RNA (%CV)[a]	6.7%	10.4%	10.0%	7.0%	6.3%	5.5%	4.3%
(-) RNA (%CV)	4.9%	10.1%	9.1%	6.3%	7.1%	6.3%	5.2%

567 [a]%CV = coefficient of variation calculated from Ct values (n = 5).
568

Figure Legends

Figure 1. False- and self-priming is common with published ZIKV qPCR primer sets. Ten-fold serial dilutions of 10^8 copies of positive-strand (A, C) or negative-strand (B, D) *in vitro* transcribed ZIKV RNA was analyzed by standard RT-qPCR using previously published ZIKV qPCR primer sets (Lanciotti *et al* 2008 (A, B) or Balm *et al* 2012 (C, D)). Specific, self- and false-priming were evaluated as described in the main text. The Ct value is plotted against the log of the RNA copy number (mean ± SEM, n = 2). Data points where amplification did not occur are not displayed on the graph.

Figure 2. Tagged primers with modified RT conditions largely eliminate false- and self-priming. (A) Tagged primer strategy for strand-specific detection of positive- and negative-strand viral RNA (vRNA). Ten-fold serial dilutions of 10^8 copies of positive-strand (B) or negative-strand (C) *in vitro* transcribed ZIKV RNA was reverse transcribed with SuperScript III Reverse transcriptase and analyzed by qPCR using tagged primers. Alternately, 10^8 copies of positive-strand (D) or negative-strand (E) *in vitro* transcribed ZIKV RNA was serially diluted 10-fold and reverse transcribed with Maxima H minus Reverse transcriptase using tagged primers. cDNA was purified prior to analysis by qPCR as described in *Materials and Methods*. Specific, false, and self-priming were analyzed as described in **Figure 1**. The Ct value is plotted against the log of the RNA copy number (mean ± SEM, n = 2). Data points where amplification did not occur are not displayed.

Figure 3. Multiplex qPCR optimization. (A) Total RNA from A549 cells infected with ZIKV was reverse-transcribed with positive- and negative-strand ZIKV tagged primers and GAPDH

592 reverse primer. cDNA was purified prior to analysis by singleplex qPCR for the indicated target,
593 or by multiplex qPCR analysis using standard PCR primer concentrations (300 nM) or primer
594 concentrations modified for multiplex qPCR as described in **Table 3**. The ΔCt of the multiplex
595 qPCR assay relative to the singleplex qPCR reaction is shown (mean ± SEM, n = 4). (B) Two-
596 hundred nanograms total RNA from A549 cells with or without 10^8 copies of both positive- and
597 negative-strand *in vitro* transcribed ZIKV RNA added was reverse-transcribed with Maxima H
598 minus reverse transcriptase and GAPDH reverse primer (total RNA only) or with GAPDH
599 reverse primer and positive- and negative-strand ZIKV tagged primers. cDNA was purified prior
600 to analysis by qPCR analysis with GAPDH primers (total RNA only) or by multiplex qPCR
601 analysis with the modified primer concentrations from panel (A) (mean ± SEM, n = 2). (C, D)
602 Ten-fold serial dilutions of 10^8 copies of the indicated *in vitro* transcribed ZIKV RNA was
603 reverse-transcribed with Maxima H minus reverse transcriptase and the corresponding tagged
604 primers (RNA alone). Alternately, ten-fold serial dilutions of 10^8 copies of both positive- and
605 negative-strand *in vitro* transcribed ZIKV RNA was mixed with 200 ng total RNA, reverse-
606 transcribed with Maxima H minus reverse transcriptase and positive- and negative-strand ZIKV
607 tagged primers and GAPDH reverse primer (RNA in multiplex). cDNA was purified prior to
608 analysis by qPCR analysis with the corresponding primer pair (RNA alone), or by multiplex
609 qPCR analysis with the modified primer concentrations from panel (A) (mean ± SEM, n = 2).
610
611 **Figure 4. Specificity of strand-specific RT-qPCR assay.** (A) 10^6 or 10^5 copies of *in vitro*
612 transcribed positive-strand RNA mixed with 10^8 copies of *in vitro* transcribed negative-strand
613 RNA was analyzed by the strand-specific assay. The ΔCt relative to 10^6 or 10^5 copies of
614 positive-strand RNA alone is shown (mean ± SEM, n = 3). (B) 10^5 or 10^4 copies of *in vitro*

615 transcribed negative-strand RNA mixed 10^8 copies of *in vitro* transcribed positive-strand RNA
616 was analyzed by the strand-specific assay. The ΔCt relative to 10^5 or 10^4 copies of negative-
617 strand RNA alone is shown (mean ± SEM, n = 4).
618
619 **Figure 5. Reproducibility of strand-specific RT-qPCR assay.** Ten-fold serial dilutions of 2.5
620 × 10^8 copies each of *in vitro* transcribed ZIKV positive-strand and negative-strand RNA was
621 analyzed by the strand-specific RT-qPCR assay. Average Ct value is plotted against the log of
622 the RNA copy number (mean ± SEM, n = 5).
623
624 **Figure 6. Representative results in mammalian and mosquito cells.** (A) JEG-3 cells were
625 infected with $ZIKV^{PR}$ (MOI 3) and RNA was harvested at the indicated time points. Positive-
626 and negative-strand viral genomes were quantified by the strand-specific RT-qPCR assay and
627 normalized to GAPDH (mean ± SEM, n = 3). (B) C6/36 cells were infected with $ZIKV^{PR}$ (MOI
628 0.01) and RNA was harvested at the indicated time points. Positive- and negative-strand viral
629 genomes were quantified by the strand-specific assay, normalized to GAPDH (mean ± SEM, n =
630 2). nd; not detected.
631

Graphical Abstract

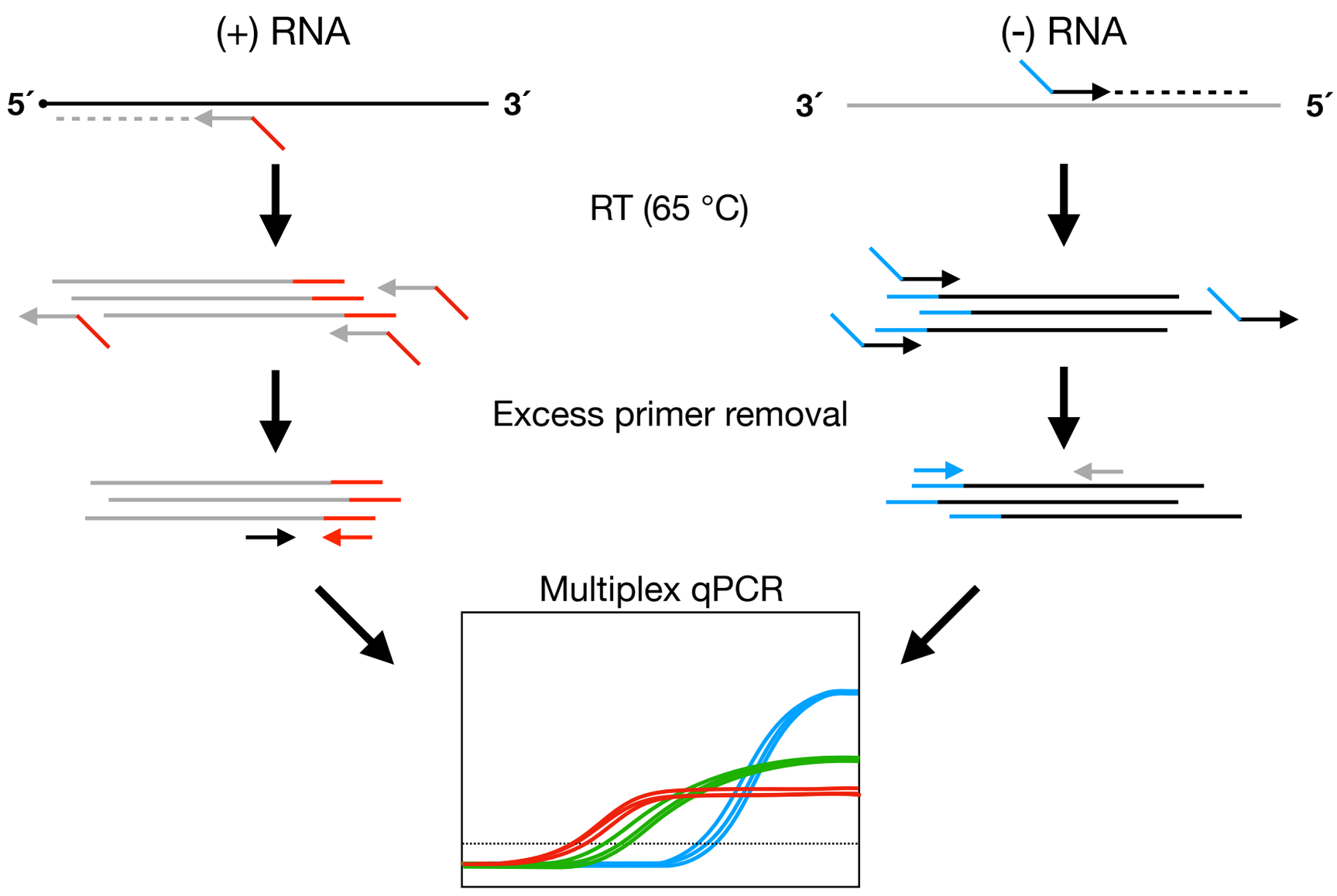

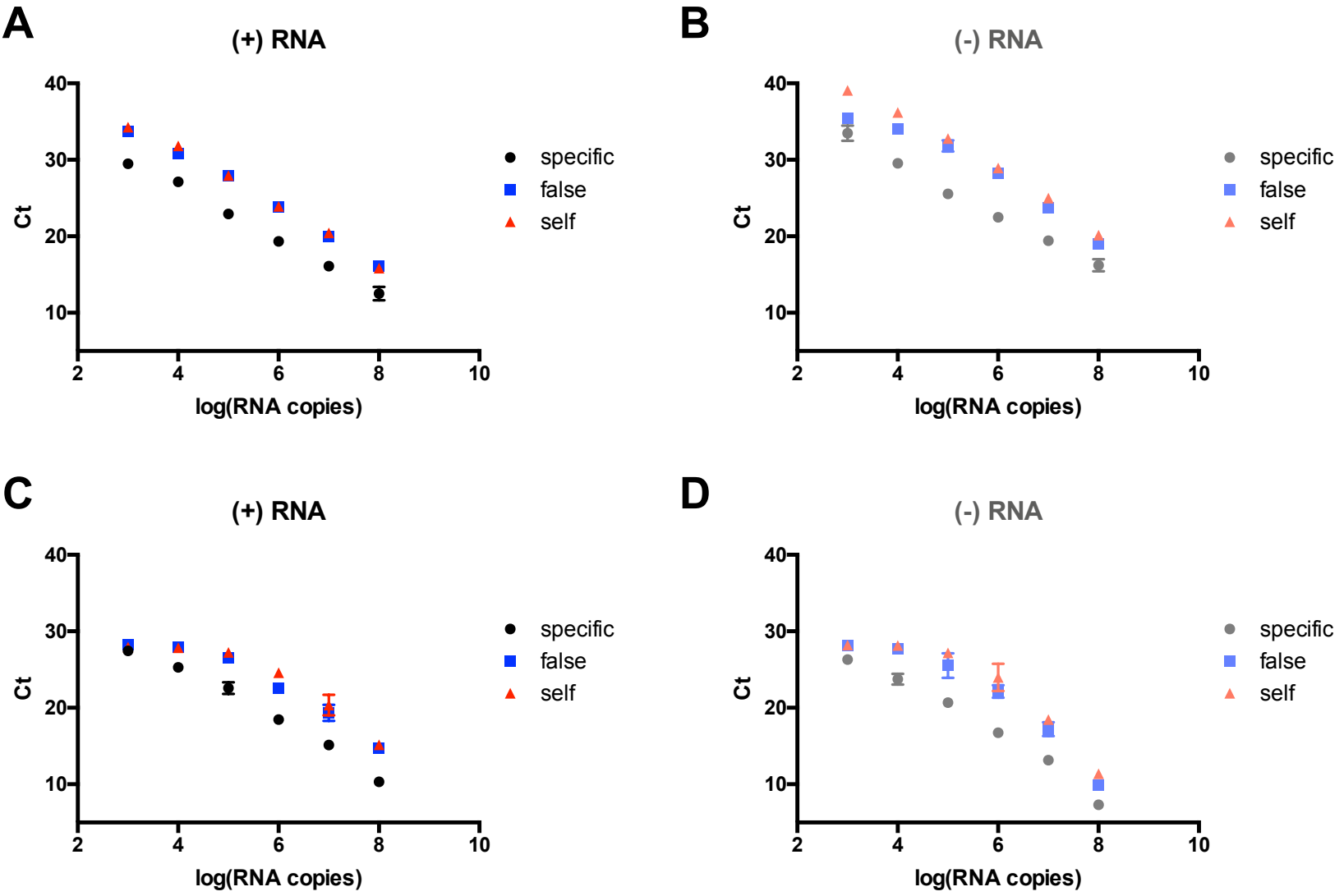
A
(+) RNA
Ct
log(RNA copies)
specific
false
self
B
(-) RNA
Ct
log(RNA copies)
specific
false
self
C
(+) RNA
Ct
log(RNA copies)
specific
false
self
D
(-) RNA
Ct
log(RNA copies)
specific
false
self

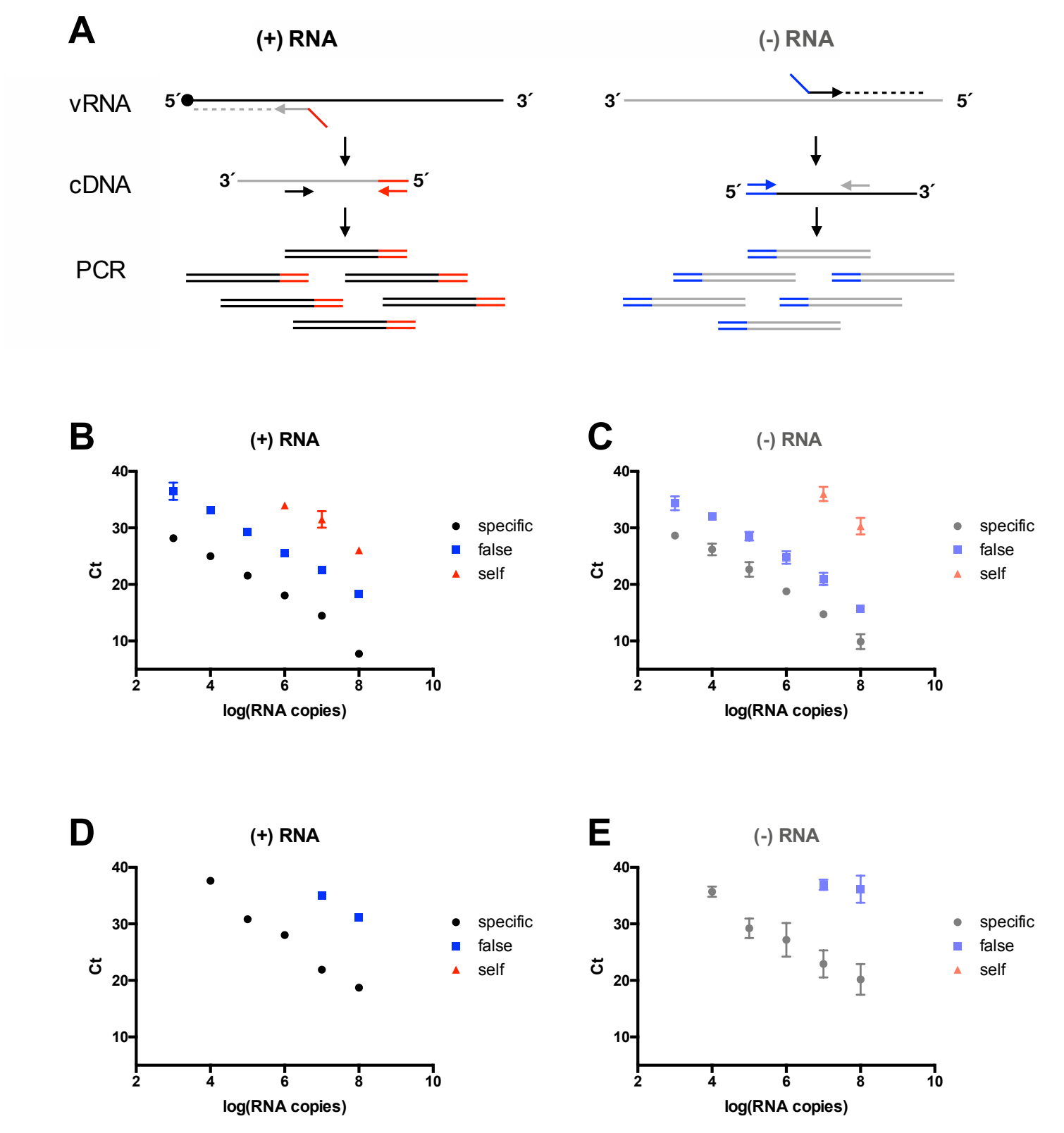
A
(+) RNA
(-) RNA
vRNA
cDNA
PCR
5´
3´
3´
5´
5´
3´
3´
5´
B
(+) RNA
C
(-) RNA
D
(+) RNA
E
(-) RNA
Ct
log(RNA copies)
specific
false
self
40
30
20
10
2
4
6
8
10

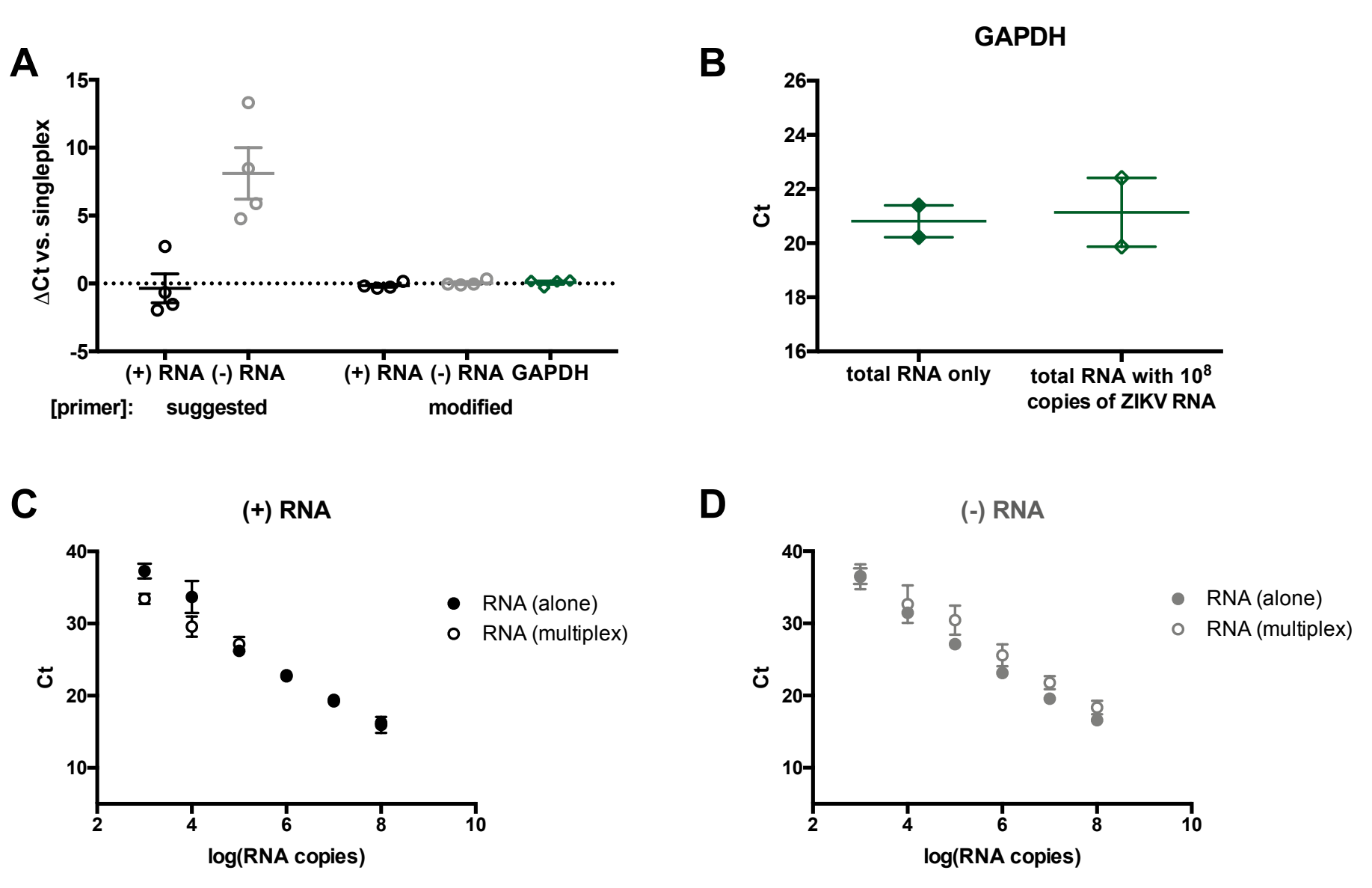
A
ΔCt vs. singleplex
15
10
5
0
-5
(+) RNA
(-) RNA
(+) RNA
(-) RNA
GAPDH
[primer]:
suggested
modified
B
GAPDH
Ct
26
24
22
20
18
16
total RNA only
total RNA with 10^8 copies of ZIKV RNA
C
(+) RNA
Ct
40
30
20
10
2
4
6
8
10
log(RNA copies)
RNA (alone)
RNA (multiplex)
D
(-) RNA
Ct
40
30
20
10
2
4
6
8
10
log(RNA copies)
RNA (alone)
RNA (multiplex)

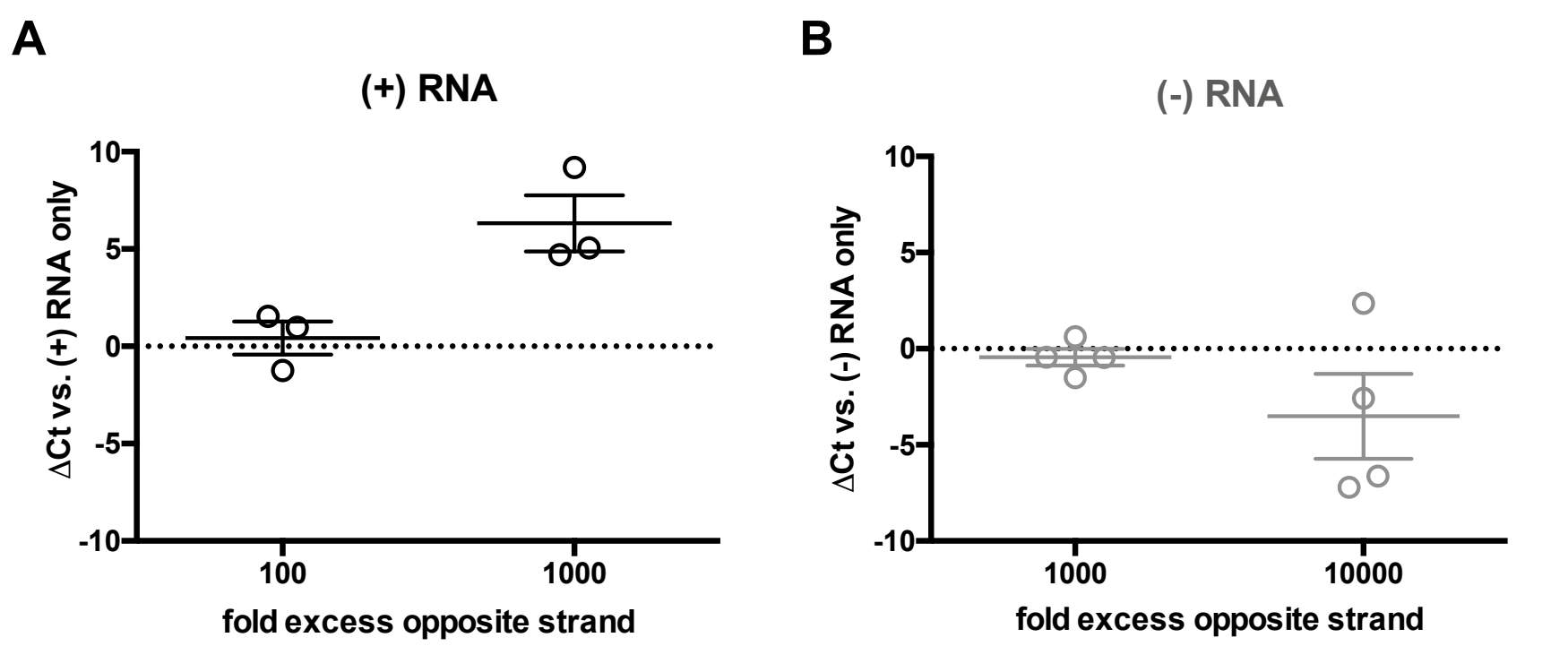
A
(+) RNA
10
5
0
-5
-10
ΔCt vs. (+) RNA only
100
1000
fold excess opposite strand
B
(-) RNA
10
5
0
-5
-10
ΔCt vs. (-) RNA only
1000
10000
fold excess opposite strand

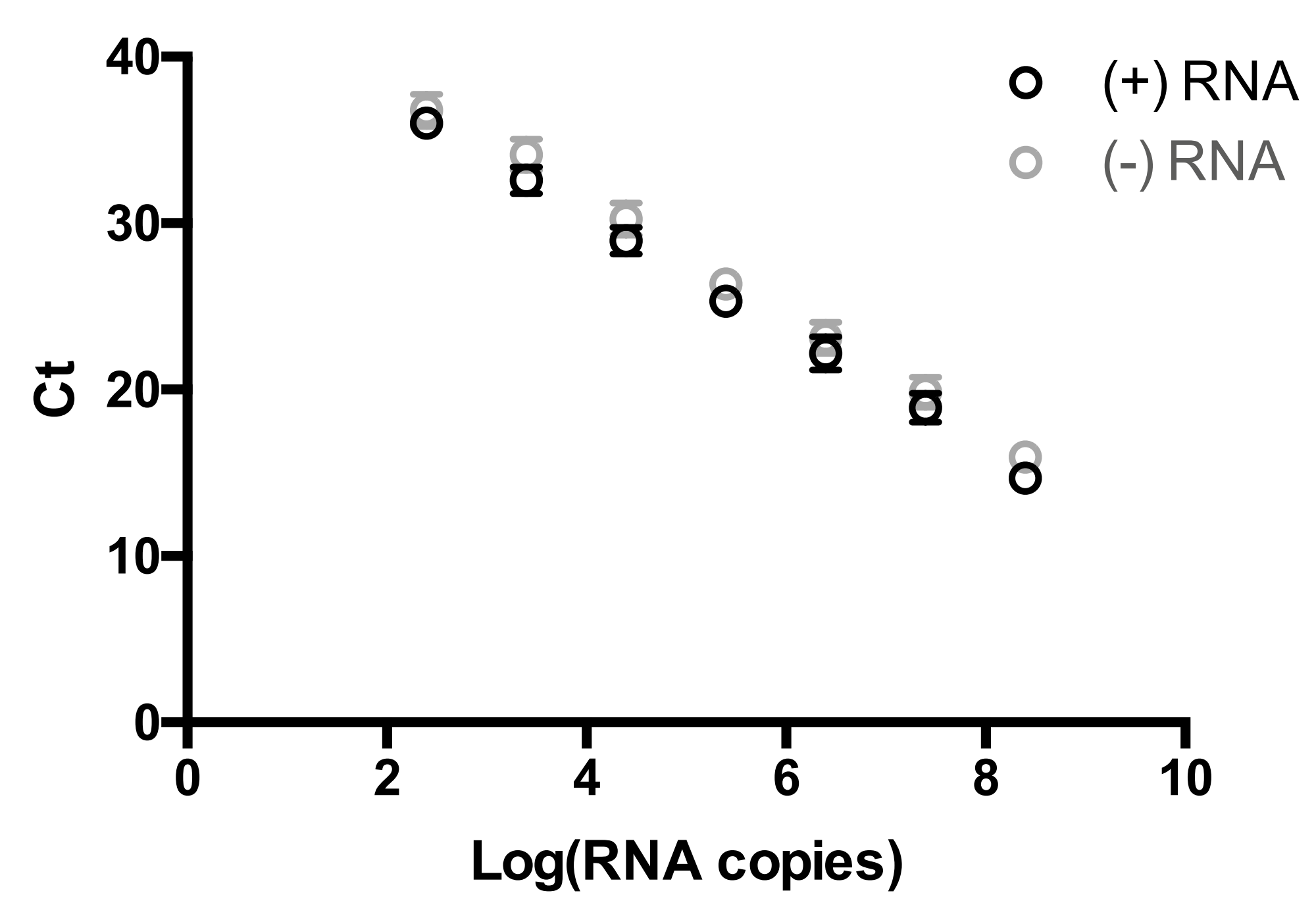
40
30
20
10
0
Ct
0
2
4
6
8
10
Log(RNA copies)
(+) RNA
(-) RNA

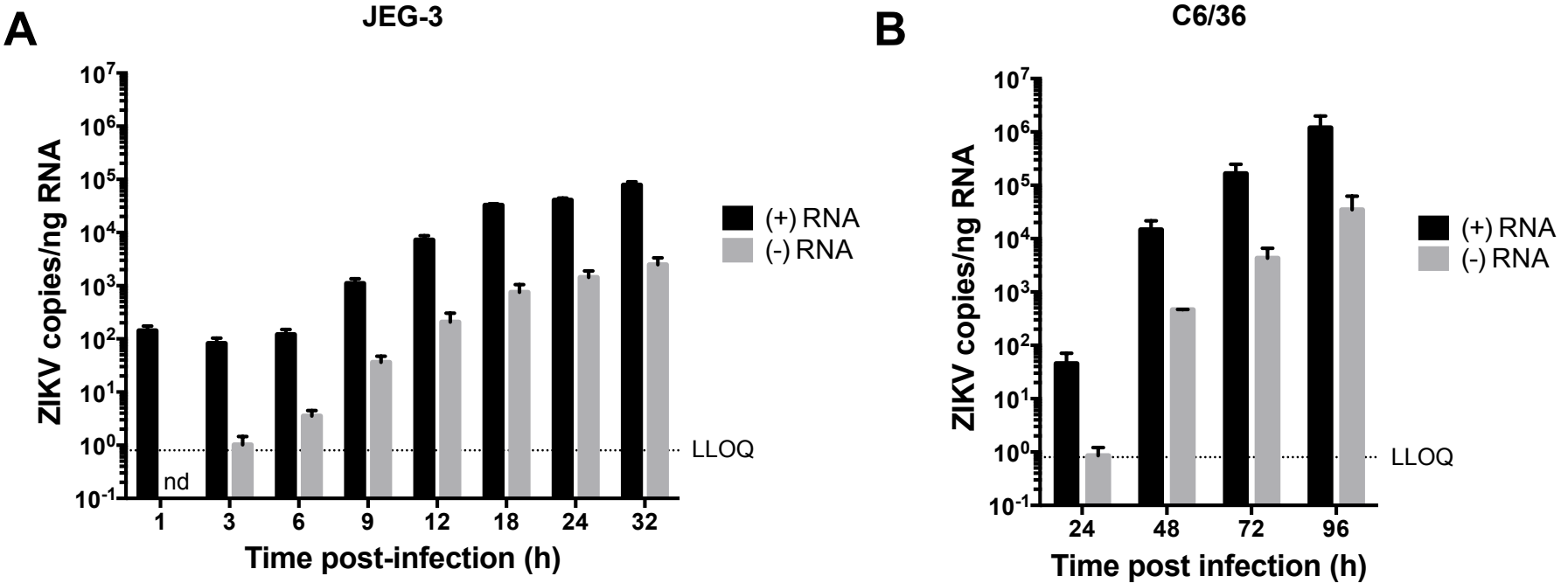
A
JEG-3
ZIKV copies/ng RNA
10^7
10^6
10^5
10^4
10^3
10^2
10^1
10^0
10^{-1}
nd
LLOQ
(+) RNA
(-) RNA
1
3
6
9
12
18
24
32
Time post-infection (h)
B
C6/36
ZIKV copies/ng RNA
LLOQ
(+) RNA
(-) RNA
24
48
72
96
Time post infection (h)